ACIDIFICATION OF FOREST SOILS:
MODEL DEVELOPMENT AND APPLICATION
FOR ANALYZING IMPACTS OF
ACIDIC DEPOSITION IN EUROPE

Pekka Kauppi
Maximilian Posch
Egbert Matzner
Lea Kauppi
Juha Kämäri

AUTHORS

Pekka Kauppi is a former research scholar of the International Institute for Applied Systems Analysis, Laxenburg, Austria. He has now returned to the Forest Research Institute in Helsinki, Finland.

Egbert Matzner is a scientific secretary of the Research Center for Forest Ecosystem/Forest Decline of the University of Göttingen in FRG.

Lea Kauppi is a former guest research scholar of the International Institute for Applied Systems Analysis, Laxenburg, Austria. She has returned to the Water Research Institute of the National Board of Waters in Helsinki, Finland.

Maximillian Posch and Juha Kämäri are research scholars at the International Institute for Applied Systems Analysis, Laxenburg, Austria.

PREFACE

The ratification of the Geneva Convention on Transboundary Air Pollution in March of 1983 showed that nations of Eastern and Western Europe were determined to control the problem of acid rain. In the same year, IIASA offered its analytical skills to the international community to help solve the problem. It did so by entering into official cooperation with the UN Economic Commission of Europe (ECE) which is responsible for implementing the convention. As part of this cooperation IIASA is developing a computer model which can be used by decision makers to evaluate policies for controlling the impact of acid rain in Europe. In addition, we hope that our work will help identify gaps in understanding the acid rain problem and stimulate the research necessary to overcome these gaps.

The IIASA model currently contains three submodels: the *Energy-Emissions* submodel, the *Atmospheric Processes* submodel and the *Forest Soil pH* submodel. The latter submodel is based on research conducted largely at the University of Göttingen (FRG). The cooperation with Professor B. Ulrich and Dr.E. Matzner is gratefully acknowledged. Background and details of the Forest Soil pH submodel are described in this Collaborative Paper, while the whole system of models has been described in a recently issued IIASA Working Paper by J. Alcamo, P. Kauppi, M. Posch and E. Runca.

Leen Hordijk
Project Leader
Acid Rain Project

ACKNOWLEDGEMENTS

SUMMARY

Acidification is considered as an unfavorable process in forest soils. Timber logging, natural accumulation of biomass in the ecosystem, and acidic deposition are known as sources of acidification. Acidification causes the risk of damage to plant roots and subsequent risk of a decline in ecosystem productivity.

A dynamic model is introduced for describing the acidification of forest soils. In one-year time steps the model calculates the soil pH as function of the acid stress and the buffer mechanisms of the soil. Acid stress is defined as the hydrogen ion input into the top soil. The buffer mechanisms counteract acidification by providing a sink for hydrogen ions. The concepts 'buffer rate' and 'buffer capacity' are used to quantify the buffer mechanisms. The model compares (i) the rate of the acid stress (annual amount) to the buffer rate, and (ii) the accumulated acid stress (over several years) to the buffer capacity. These two types of comparisons produce an estimate of the soil pH as the output.

The model was incorporated into a model system for analyzing the acidic deposition problem in Europe. The data on acid stress, entering the soils, was obtained from other submodels which link information on energy production, pollutant emission, pollutant transport, and pollutant deposition. Data on buffer rate and buffer capacity were collected from soil maps and geological maps.

The model system as a whole is now available for analyzing different emission scenarios. The soil acidification model assumes sulfur deposition estimates from the other submodels as the input, and as the output it produces estimates of the pH of European forest soils in a map format. Additionally it computes the total area of forests in Europe with the estimated soil pH lower than any selected threshold value. Sources of uncertainty of the soil acidification model are listed and briefly evaluated.

CONTENTS

ACIDIFICATION OF FOREST SOILS:
MODEL DEVELOPMENT AND APPLICATION
FOR ANALYZING IMPACTS OF
ACIDIC DEPOSITION IN EUROPE

Pekka Kauppi
Maximilian Posch
Egbert Matzner
Lea Kauppi
Juha Kämäri

1. Introduction

1.1. Acidification and Forest Damage

Forest damage has been observed in rural areas in Central Europe to a large extent since the 1970's. It was first reported on silver fir (Schütt, 1977) and later on Norway spruce, Scots pine, beech, and other tree species as well (Schütt et al., 1983). In 1982 damage was reported on forest area of 560,000 ha in the Federal Republic of Germany. Recent results suggest that by the year 1983 the area of damage in FRG has considerably enlarged (Lammel, 1984).

Air pollution is generally considered as a major reason for forest damage. Two physiological pathways have been identified: (i) Direct action of pollutants on the leaves and the subsequent decline of photosynthetic productivity; and (ii) Root damage due to unfavorable

changes in the soil. Soil acidification is associated with the latter pathway.

Protective measures against air pollution damage, including forest damage, are being planned under the auspices of the ECE Convention on Long Range Transport of Air Pollution in Europe. IIASA's Acid Rain Project has the general objective of developing models which would assist in comparing the benefits of different control options. This study is part of that effort. It addresses soil acidification which may result, for example, from the accumulation of forest biomass but which is also an important link between air pollution and forest damage.

1.2. Objectives of the Study

The study includes method development and method application. The main objective of the study is to develop a method for computing the time evolution of acidification of forest soil. An additional objective is to apply the method for getting an overview of the forest soil acidification in Europe due to air pollution.

2. Model Development

2.1. Soil Acidification

2.1.1. Process of Soil Acidification

Soil acidification has been defined as being a decrease in the acid neutralization capacity of the soil (van Breemen et al. 1984). Such a decrease may coincide with a decrease in the soil pH. It may also take place in conditions of a relatively constant pH assuming efficient buffer-

ing processes. In such a case the buffering of the soil counteracts the effect of acidic deposition or biomass removal, so that over long periods of time the soil pH is stabilized at a constant level. Yet the neutralization capacity is being consumed and the soil is subject to acidification.

2.1.2. Acid Stress

Acid stress is defined as the input of hydrogen ions (protons) into the top soil. Acid stress can result from acidic deposition of air pollutants, from biomass utilization, and from the natural biological activity of ecosystems (Ulrich, 1983a; van Breemen et al., 1984). Any one of these sources can dominate the stream of protons entering the soil. The acid stress due to air pollution can result from the direct deposition of hydrogen ions or from the indirect effect of acid producing substances such as the dry deposition of SO_2.

Acid stress has two important aspects. One is the accumulative load of the stress and the other is the instantaneous rate of the stress. The variable *amount of stress* refers to the load, and involves accumulation over several years. The unit for the amount of stress is kiloequivalents of acidity per hectare (keq ha^{-1}). The variable *stress rate* refers, in principle, to the time derivative of the 'amount of stress' although in practice it is given as annual hydrogen ion input. The unit for the stress rate is kiloequivalents of acidity per hectare and year (keq $ha^{-1}yr^{-1}$).

2.1.3. Buffering Processes

Soil reacts to the acid stress depending on the soil properties. Acid stress implies influx of hydrogen ions, and in the corresponding way the *buffering properties of the soil* imply consumption of hydrogen ions. Buffering is described using two variables, one for the gross potential and the other for the rate of the reaction. Both variables refer to the intrinsic properties of the soil. They can be quantified after fixing the volume of the reacting soil layer.

Buffer capacity, the gross potential, is the total reservoir of the buffering compounds in the soil. The unit for the buffer capacity is the same as that for the amount of the acid stress ($keq\ ha^{-1}$).

Buffer rate, the rate variable, is defined as the maximum potential rate of the reaction between the buffering compounds and the hydrogen ions. This variable is needed because the reaction kinetics sometimes restrict the rate at which hydrogen ions are consumed. Although the buffer capacity is high this maximum rate sometimes limits the hydrogen ion consumption. Buffer rate can be expressed in units which are comparable to those of the stress rate ($keq\ ha^{-1}yr^{-1}$).

2.1.4. Buffer Ranges

The proton consumption reactions in soils have been systematically described by Ulrich (1981, 1983b). A consecutive series of chemical reactions has been documented in soils in which the acidification proceeds. Information regarding the dominant reactions has been used for defining categories, called *buffer ranges*. They are briefly described in the following paragraphs and summarized in Table 1. The name of each buffer

range refers to the dominant buffer reaction.

Carbonate buffer range

Soils containing $CaCO_3$ in their fine earth fraction (calcareous soils) are classified into the carbonate buffer range (pH > 6.2). Ca^{2+} is the dominant cation in the soil solution and in the exchange surfaces of the soil particles. The buffer capacity of soils in this range is proportional to the amount of $CaCO_3$ in the soil. In case $CaCO_3$ is evenly distributed in the soil, the buffer rate, i.e. the dissolution rate of $CaCO_3$, is high enough to buffer any occurring rate of acid stress.

Silicate buffer rate

If there is no $CaCO_3$ in the fine earth fraction and the carbonic acid is the only acid being produced in the soil, the soil is classified into the silicate buffer range (6.2 > pH > 5.0). In this range the only buffer process acting in the soils is the weathering of silicates. The buffer rate is often quite low. The buffer capacity, in turn, is high as it is formed by the massive storage of the silicate material.

Cation exchange range

When the cation exchange reactions play the major role in the acid buffering, the soils are classified into the cation exchange buffer range. This implies that the silicate buffer range is not capable of buffering the acid stress completely. The excess stress, not buffered by the reactions of the silicate buffer range, is adsorbed in form of H^+ or Al-ions at the exchange sites, thus displacing the base cations. The cation exchange reactions are fast and, therefore, the buffer rate of soils in this range effectively counteracts any occurring rates of the acid stress. The buffer

capacity (= cation exchange capacity, CEC) is generally rather low depending mainly on the soil texture. The remaining buffer capacity at any given time is quantified by *base saturation*, the percentage of base cations of the total CEC. As long as the base saturation stays above 5-10 percent, the excess stress is buffered by the cation exchange reactions and the soil pH takes a value between 5.0 and 4.2, the actual value depending linearly on the base saturation.

Aluminum buffer range

Below the critical value of base saturation the soils are classified into the aluminum buffer range. Hydrogen ions are consumed in releasing aluminum mainly from clay minerals. These reactions merely change the form of acidity from hydrogen ions to Al^{3+}. The leachate thus has a potential of acidifying the adjacent ecosystems. High aluminum ion concentrations characterize the soil solution and may cause toxic effects to the bacteria and plant roots. The soil pH is within the range 4.2-3.0.

Aluminum compounds are abundant in soils, so that the buffer capacity hardly ever restricts the reaction. Buffer rate is decisive: The soils do not fall below the aluminum buffer range until the stress rate exceeds the production rate of highly dissolvable Al hydroxo compounds.

Iron buffer range

At the extreme stage of acidification soils are classified into the iron buffer range. High solubility of iron oxides is observed. The pH values as low as < 3.0 indicate toxicity and nutrient deficiency to living organisms.

Table 1: Classification of the acid buffering reactions in forest soils (Ulrich, 1981,1983b)

Buffer range	Typical pH	Buffer reaction
Carbonate	8.0-6.2	$CaCO_3 + H_2O + CO_2(g) \rightarrow Ca^{2+} + 2HCO_3^-$
Silicate	6.2-5.0	$CaAl_2Si_2O_8 + 2H_2CO_3 + H_2O \rightarrow$ $Ca^{2+} + 2HCO_3^- + Al_2Si_2O_5(OH)_4$
Cation exchange	5.0-4.2	clay mineral=Ca + $2H^+ \rightarrow$ H-clay mineral-H + Ca^{2+}
Aluminum	4.2-3.0	$AlOOH + 3H^+ \rightarrow Al^{3+} + 2H_2O$
Iron	<3.8	$FeOOH + 3H^+ \rightarrow Fe^{3+} + 2H_2O$

2.2. Structure of the Model

The model describes soil acidification in terms of the sequence of the buffer ranges. The model compares i) the amount of stress (cumulative value over the time period of interest) to the the buffer capacity, and ii) the stress rate (year-to-year basis) to the buffer rate. The comparisons - which are simple because the buffer variables and the stress variables are expressed in compatible units - are done separately for each buffer range. The model thus assumes that the values for the soil variables -- buffer capacity and buffer rate -- are determined separately for each buffer range.

The number of potential soil variables would be ten as there are five buffer ranges. Some of these variables are, however, irrelevant. For example, the buffer rates of the carbonate range and the cation exchange range are so high that in practice they can not be exceeded by any occurring rate of acid stress. Moreover, the buffer capacities of

silicate and aluminum ranges can not be exhausted in the time scale of hundreds of years. Soil variables for the iron range are assumed high since this range has been described as the extreme stage of soil acidification.

In this way the number of variables actually included into the model reduces to four. The excluded six variables receive values high enough not to affect the model output (Table 2).

Table 2:   The variables included in the model

Buffer range	Buffer capacity	Buffer rate
Carbonate	BC_{Ca}	--
Silicate	--	br_{Si}
Cation exchange	BC_{CE}	--
Aluminum	--	br_{Al}
Iron	--	--

The model hence assumes quantitative initial values for the four variables indicated in Table 2. The model runs by taking the given pattern of acid stress as the input variable. The program compares the (annual) acid stress to the buffer rate which is typical of the prevailing buffer range. It also compares the accumulated amount of the acid stress to the buffer capacity. With these comparisons the program calculates which buffer range prevails each year, and then converts this information into an approximation of the prevailing soil pH (Figure 1).
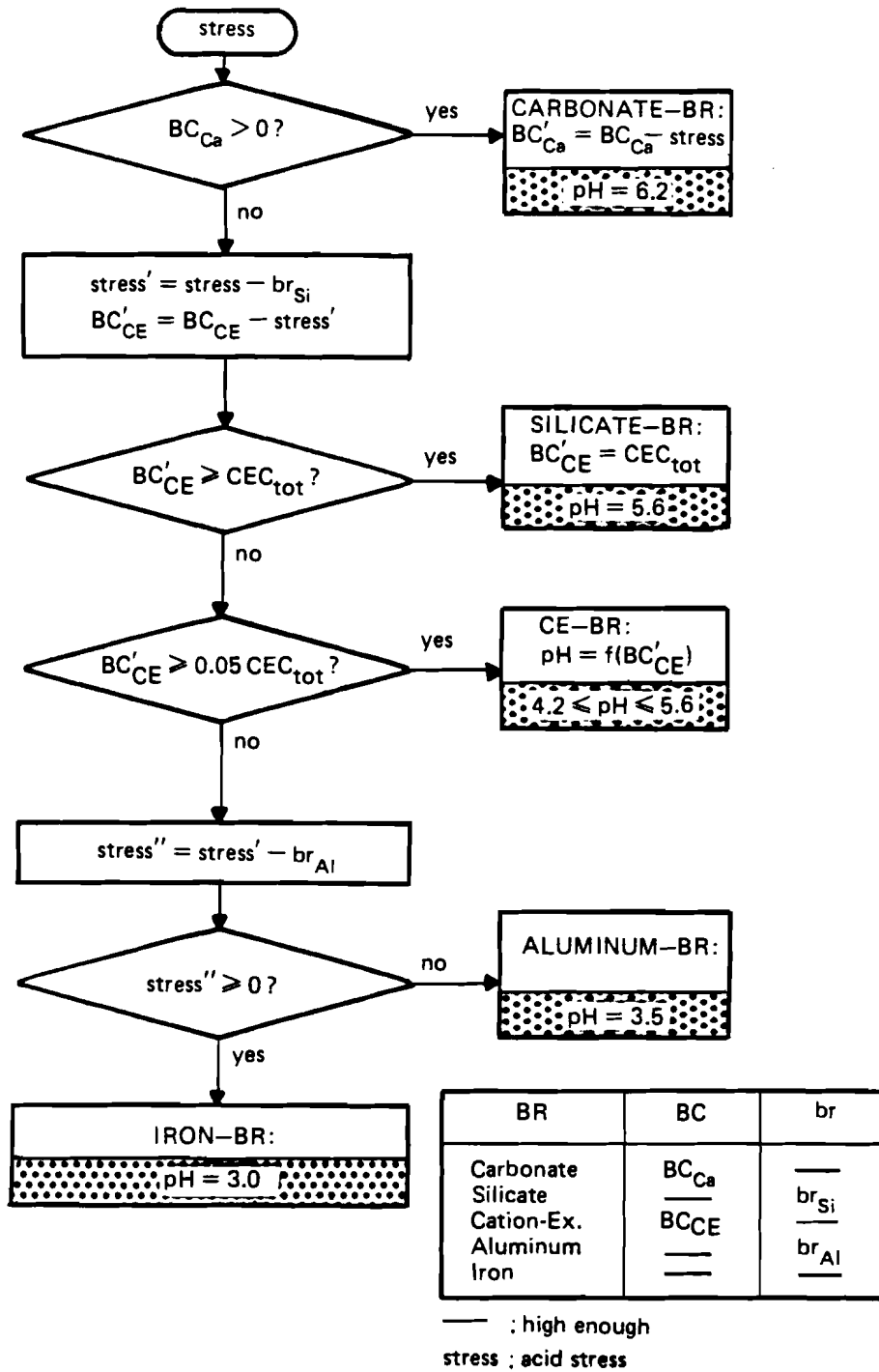
Figure 1. Flow diagram of the soil acidification model.

2.3. Model Demonstration

The dynamic features of the model are demonstrated in this section by producing a series of input-output figures. The estimated time evolution of the soil pH is depicted as a function of four different patterns of acid stress. These input-output figures describe the reactions of only one soil type. Table 3 indicates the soil characteristics assumed to prevail in the beginning of the 100 year study period.

Table 3:   Initial values for the variables of the example soil

Buffer range	Buffer capacity (keq ha^{-1})	Buffer rate $(\text{keq ha}^{-1}\text{yr}^{-1})$
Carbonate	$BC_{Ca} = 0.0$	--
Silicate	--	$br_{Si} = 2.0$
Cation exchange	$BC_{CE} = 90.0$	--
Aluminum	--	$br_{Al} = 2.0$
Iron	--	--

BC_{Ca} being zero indicates that this example deals with a soil free of lime. When fixing these values the reacting soil layer was assumed to be 50 cm thick. The value for the buffer rate of the silicate buffer range is somewhat high for such a shallow soil layer. However, this only affects the time scale of the acidification not the qualitative behavior of the model which is the subject of this demonstration.

The input of this model demonstration consists of four hypothetical time patterns of the acid stress for the period of 100 years. The output is the time pattern of the soil pH, corresponding to the mean hydrogen ion concentration of the soil layer of 50 cm.

Figure 2 indicates that the soil pH remains at a constant level of 5.6 when the soil is subject to a constant, low-level stress $(1 \text{ keq ha}^{-1}\text{yr}^{-1})$. The pH is predicted this low because no capacity is available in the carbonate range. (The pH 5.6 was selected as a typical pH value within the silicate buffer range.) The buffering is due to the processes of the silicate buffer range. Constant pH results because the rate of the acid stress, $1 \text{ keq ha}^{-1}\text{yr}^{-1}$, is lower than the buffer rate of the silicate range, $2 \text{ keq ha}^{-1}\text{yr}^{-1}$.

Increasing the acid stress to $3 \text{ keq ha}^{-1}\text{yr}^{-1}$ yields a decline of the soil pH from 5.6 to 4.2 (Figure 3). Processes of the silicate buffer range account for the buffering of two thirds of the acid stress. The remaining 1 keq $\text{ha}^{-1}\text{yr}^{-1}$ is buffered by the processes of the cation exchange range. After the buffer capacity of the cation exchange range is exhausted the aluminum buffer range comes into effect. The soil pH is stabilized at 3.5 because the buffer rate of the aluminum range $(2 \text{ keq ha}^{-1}\text{yr}^{-1})$ is higher than the acid stress which remains in the soil after the buffering of the silicate range. (The value 3.5 was selected as a typical pH within aluminum buffer range). This example indicates that the buffering within the silicate buffer range, essentially due to the weathering of the silicate minerals, is modeled active through all the buffer ranges.
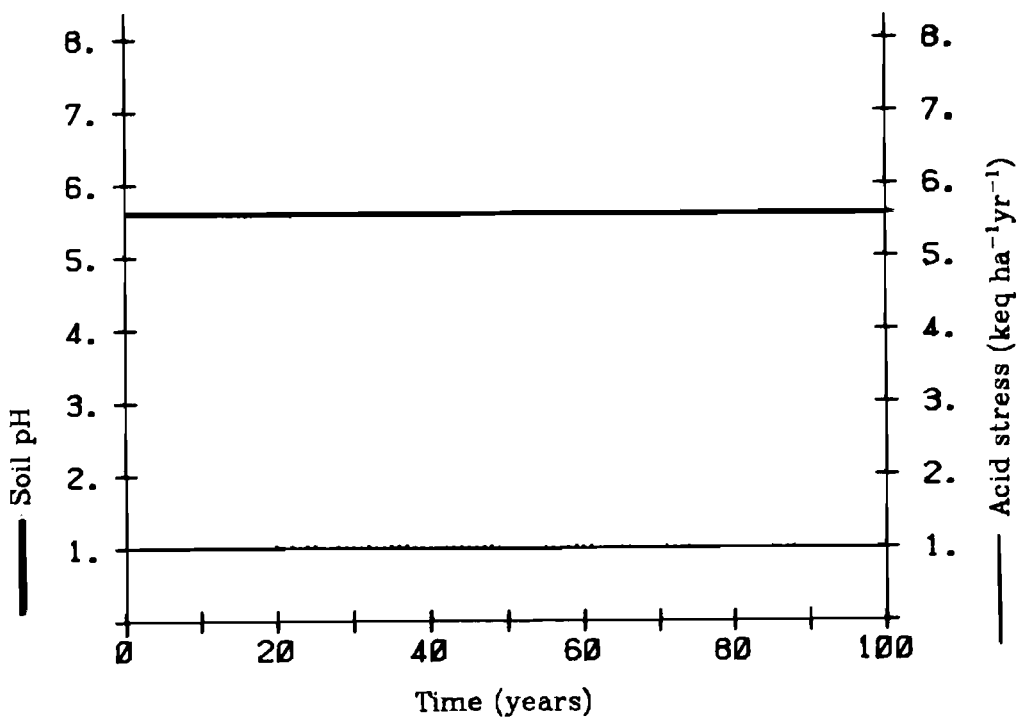
Figure 2. Input-output relationship: response of the soil to a low, constant stress.
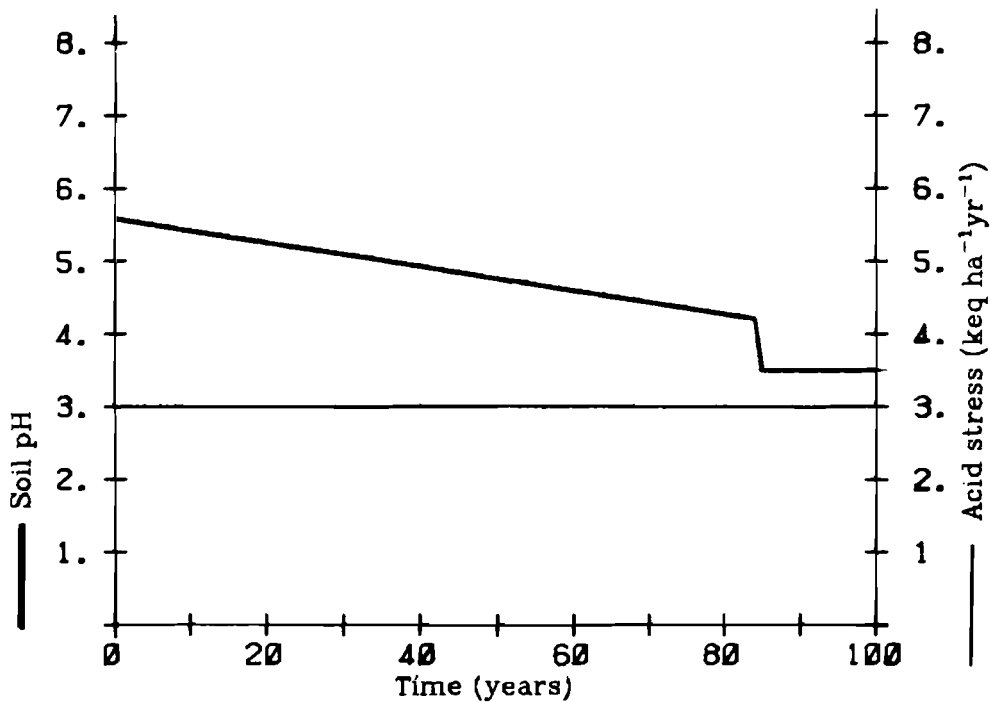
Figure 3. Input-output relationship: response of the soil to a high, constant stress.

The decline from pH 5.6 to pH 4.2 occurs gradually (Figure 3). This feature was included because of the character of the processes in the cation exchange range. The hydrogen ions gradually replace the base cations on the exchange sites of the soil particles thus decreasing the base saturation of the soil. This has to do with the equilibrium between the ions attached to the soil particles and those dissolved in the soil solution. A linear relationship is assumed between the base saturation and the pH within the cation exchange range at pH from 5.6 to 4.2. The gradual character was introduced also for the recovery. The recovery of the soil follows the decline in the acid stress with a delay (Figure 4).

Introduction of a growing stress rate reveals an additional feature of the model (Figure 5). When the acid stress is high (>4 keq ha^{-1}yr^{-1}) the model predicts an abrupt decline in the soil pH to the level of the iron buffer range (3.0). This is due to several reasons:

1)   There is no buffer capacity in the carbonate buffer range,

2)   The rate of acid stress exceeds the buffer rate of the silicate buffer range,

3)   The buffer capacity of the cation exchange range is exhausted,

4)   The rate of acid stress, although partly buffered within the silicate buffer range, exceeds the buffer rate of the aluminum range.

Since none of the higher buffer ranges is capable of buffering the stress, the pH declines to the level which corresponds the characteristic pH of the iron buffer range.
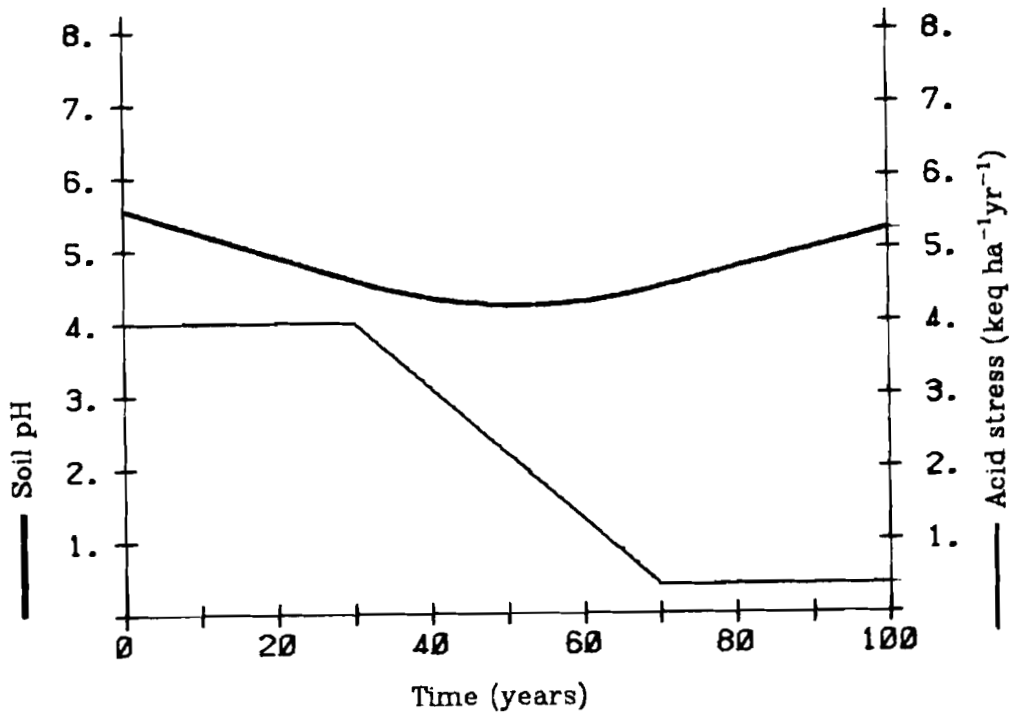
Figure 4. Input-output relationship: response of the soil to a declining stress.
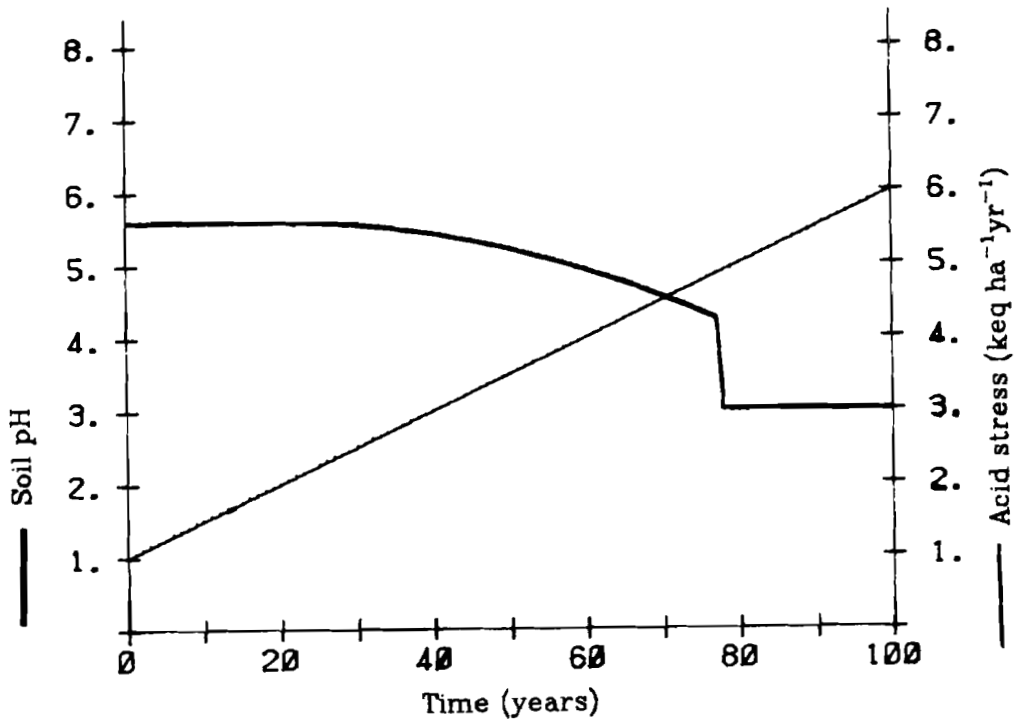
Figure 5. Input-output relationship: response of the soil to an increasing stress.
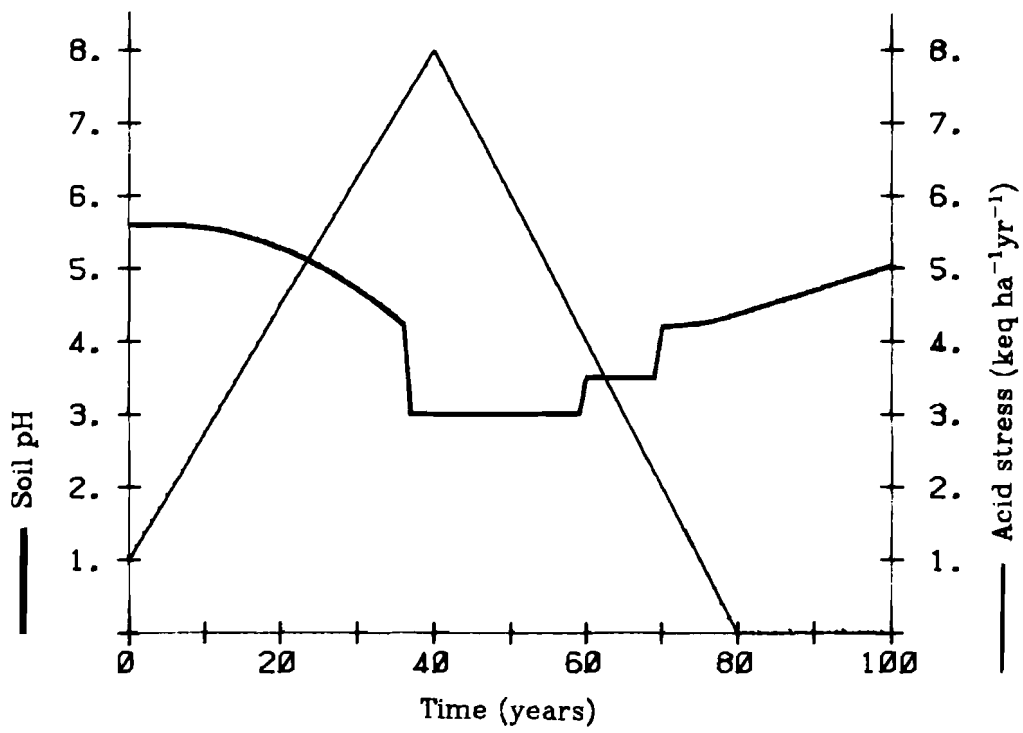
Figure 6. Input-output relationship: a summary of the model behavior;
see text for explanation.

A dramatic pattern of the acid stress is selected to summarize the dynamic behavior of the model (Figure 6). The pattern includes an increase of the acid stress from 1 keq $ha^{-1}yr^{-1}$ to 8 keq $ha^{-1}yr^{-1}$ in 40 years and a linear decline to zero in the subsequent 40 years. The remaining 20 years exhibit zero stress. The soil with initial conditions as in Table 3 reacts in the following way. First, there is a short period of constant pH at 5.6. The buffer rate of the silicate buffer range is higher than the acid stress. Next, there is a gradual but accelerating decline in pH from 5.6 to 4.2. The increasing acid stress consumes the buffer capacity of the cation exchange range at an accelerating rate. Next, there is a rapid decline of pH to the iron buffer range, that is, to pH 3.0. The buffer capacity of the cation exchange range is exhausted and the buffer rate of the aluminum range cannot keep the pace with the rate of the acid stress. Next, there is an increase of the soil pH to 3.5. At that point the acid stress has declined so that the joint buffering of the silicate buffer range and the aluminum range is capable of stabilizing the pH. Finally, a recovery starts from pH 3.5 upwards. This is possible because the acid stress is at a level where the silicate buffer rate is sufficient for buffering the stress alone. The cation exchange capacity is refilled, starting at pH 4.2, with a rate equal to the difference of the buffer rate of silicate buffer range and the rate of the acid stress. The full base saturation, however, will not be reached by the end of the 100 year period.

3. Model Application

3.1. The IIASA context

This application is part of the IIASA Acid Rain Study which has the general objective of analyzing alternative control strategies of the European sulfur emissions. The focus of the application is hence restricted to the stress due to air pollution. The IIASA framework sets the prerequisite of a large spatial scale. According to the model structure two aspects need to be quantified: the acid stress and the buffering processes.

3.2. Estimating Acid Stress

Direct estimates and models are lacking which would describe the acidic deposition in the scale of Europe in terms of acid stress. However, sulfur deposition has been monitored and modeled, for example, within the EMEP-program (OECD, 1979). A conversion factor was used for transforming the sulfur deposition, kg ha^{-1}, to the acid stress, keq ha^{-1}. This factor (1/16) is simply the ratio of H to S in sulfuric acid. This simplification made it possible to generate rough estimates of acidic deposition over such a wide area as Europe.

The IIASA project has provided an energy-emission model for generating scenarios of future sulfur emission for Europe assuming optional programs for energy development and sulfur control (Alcamo et al. 1984). The computed emissions are converted into sulfur deposition scenarios by using the long-range transport model for air pollutants developed within the EMEP-program. Sulphur deposition is then

transformed into an approximation of the acid stress, and this information is used as the input variable of the soil acidification model.

3.3. Estimating the Buffering Variables

Initialization of the soil variables was based on the chemistry information available on European soils. The buffer capacity of the carbonate range is proportional to the lime content of the soil; the buffer rate of the silicate range is related to the chemical weathering rate of the silicate minerals; the buffer capacity of the cation exchange rate depends on the clay content and on the base saturation of the soil; and the buffer rate of the aluminum range depends on the accessability of aluminum compounds. Although such relationships, especially those regarding the Al accessability are only partially understood, they can be used as a guideline in quantifying the susceptibility of the soils to acidification. The values for the buffer capacities and buffer rates were initialized accordingly based on the International Geological Map of Europe and the Mediterranean Region (1972) and the FAO-Unesco Soil Map of the World (1974). The depth of the reacting soil was assumed 50 cm throughout the study area. The year 1960 was selected as being the baseline year.

All information regarding soils was stored into a computerized grid-based format. Each grid square has the extension of 1 degree longitude times 0.5 degrees latitude. In this way the size of a grid was fixed at 56 km in the south-north direction, but in the east-west direction it varied from 91 km to 38 km depending on the latitude. The number of the grid squares is 2473.

Detailed soil chemistry information regarding the other soil variables was available from the Soil Map. The resolution of the map is such that the standard grid square was composed of 1-7 soil types. (The number of different soil types was 82). The fraction of each soil type within the grid square was computerized with an accuracy of 5 per cent units. An initial values for the soil variables were given for every soil type (Appendix 1).

The Soil Map, however, could not provide the information regarding the buffer rate of the silicate buffer range which is equal to the weathering rate of the parent material. The approximation of this variable was based on other sources. Ulrich (1983b) reports a range of variation in European soils from 0.2 to 2.0 keq $ha^{-1}yr^{-1}m^{-1}$. Four classes for the reacting 50cm soil layer were introduced with the following buffer rates (in keq $ha^{-1}yr^{-1}$):

class	1	2	3	4
buffer rate	0.25	0.50	0.75	1.00

The Geological Map was used to determine parent materials of soils in each grid square. Depending on the dominant parent material the soil of each grid square was classified into one of the above categories (Appendix 2).

Based on this information the model is applicable for producing acidification scenarios for forest soils. The model is run separately for each soil type within the grid square. An estimate of the soil pH is produced as the output. An average pH is calculated for each grid square by weighing it by the fraction of the soil type. This pH is then the output of the

model for that grid square.

3.4. Results of Model Runs

Two example scenarios were introduced using the IIASA energy-emission model, and the long range transport model supplied by the EMEP project. From 1960 until 1980 the scenarios were identical. From that on the scenarios departed so that the 'low' deposition scenario assumed low rates of energy development throughout Europe and, in addition to that, effective measures taken for the control of the sulfur emissions. The 'high' deposition scenario was constructed by modifying the assumption to bring about higher sulfur emission (Figure 7). The two scenarios assume that sulfur emissions are changed proportionally in all grid squares. The baseline distribution is fixed using data from an inventory conducted in 1974. The specific method of generating different scenarios is presented elsewhere (Alcamo et al. 1984).

The model can be used for producing an estimate of the pH of forest soils for any selected scenario and year (Figure 8). An option has been added for simplifying the output format by introducing a concept 'critical pH'. This concept bears on the notion that the risk of forest damage increases below that threshold value. A default value of 3.5 was introduced for the critical pH but the model user can interactively select other values. The area below the critical pH is displayed in map format (Figure 9).

For summarizing the results an option has been added to display esti mates of the time patterns of the total forest area with soils below the critical pH (Figure 10). Data was needed for this option on the fraction of forests, as opposed to other land uses, in each grid square. This data was
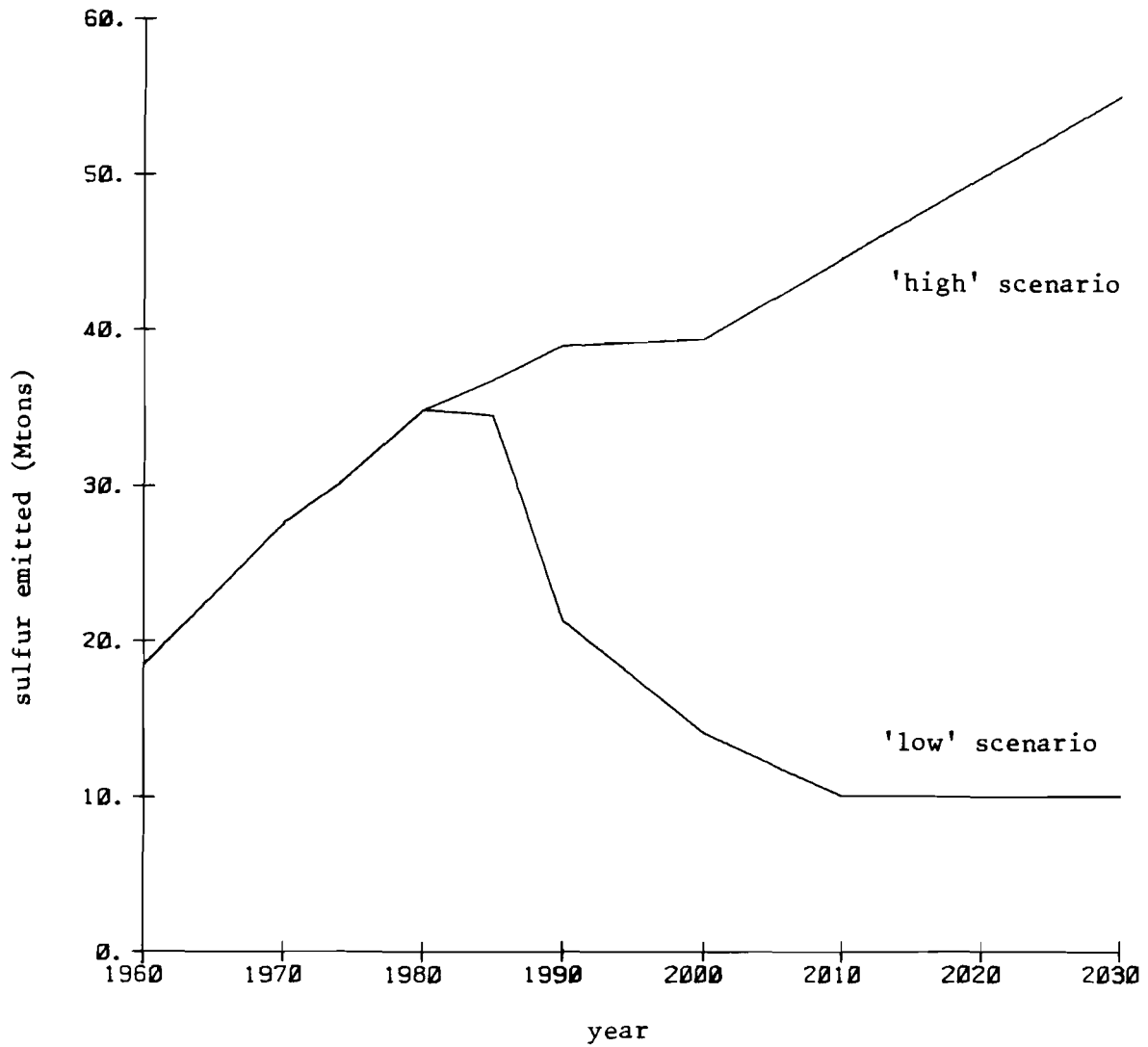
Figure 7. Total sulfur emitted in Europe according to the 'high' and 'low'
emission scenario.
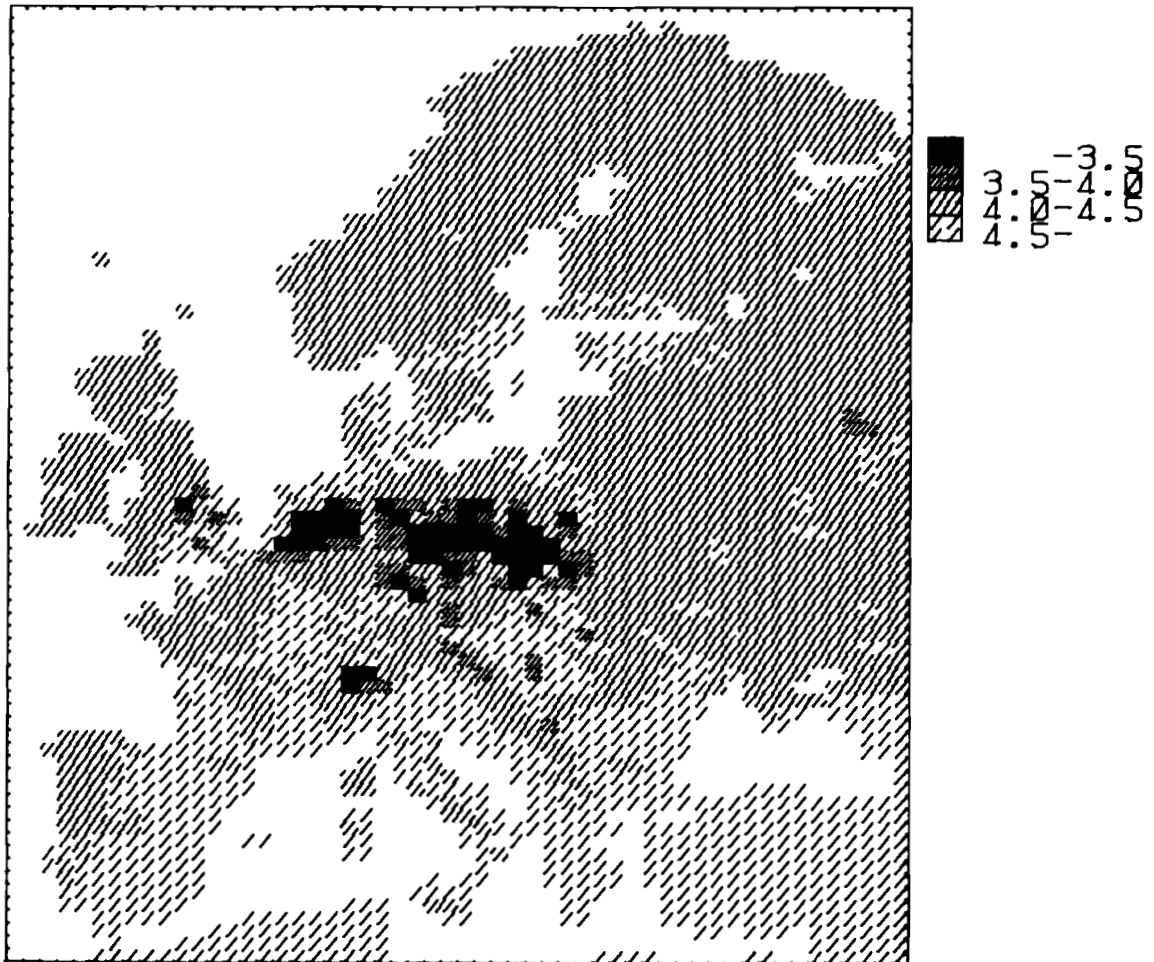
Figure 8. Model estimates of the soil pH in Europe in 1980.
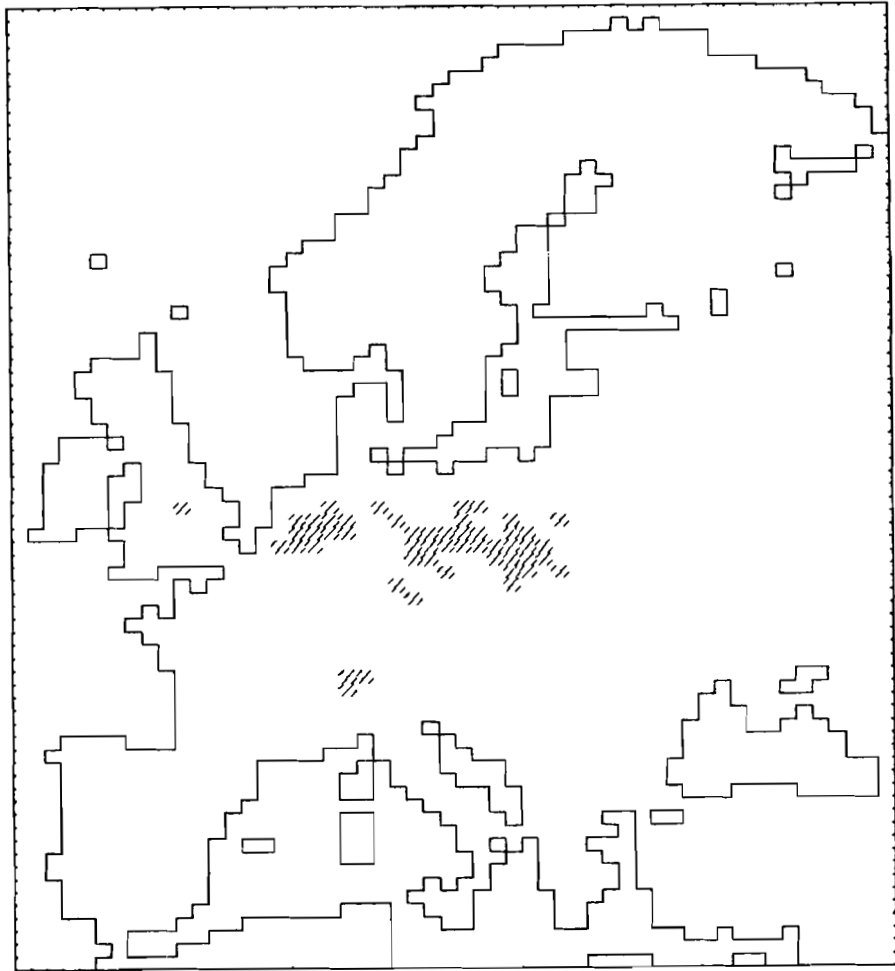
Figure 9. Model estimates of forest soils below pH 3.5 in 1980.

obtained from the World Forestry Atlas (Weltforstatlas, 1975). The procedure of calculating the total forest area below the critical pH includes the following phases. First, the size of the grid square is calculated (this varies with latitude). The size is then multiplied by the fraction of forests yielding an estimate of the area of forests in the grid square. Average soil pH is calculated for the grid square, and the results on forest area and on average soil pH are aggregated from all grid squares. The procedure relies on the assumption that the forests within the grid square are evenly distributed among all soil types.

As part of the IIASA study this application of the soil acidification model is designed for quick comparisons of sulfur emission scenarios. It is up to the model user to decide what kind of scenarios should be compared. The two examples were selected to demonstrate the model behavior. Therefore, the examples are relatively useless as far as selecting feasible policy options is concerned. The following paragraphs discuss the effects of the 'low' vs. the 'high' scenario but this discussion is intended merely to demonstrate the properties of the model.

By the year 1980 that is, assuming the more or less historical deposition pattern, the model predicts a decline in the soil pH in relatively large regions of Central Europe. Continuing with the 'high' deposition scenario the area of low pH substantially enlarges by the year 2010 and much of the soils in Central Europe reaches the iron buffer range. Yet, although assuming the high scenario, the soil pH in much of the Nordic countries remains essentially unchanged (Figure 11).

The region where the soils fall below pH 3.5 appears on the map already by 1973 (Figure 12). This area, interpreted as the area of risk of forest damage, increases by 1980 (Figure 9) and, with the 'high' deposition scenario, it further substantially enlarges by the year 2010 (Figure 13). When the 'low' deposition scenario is used as the input, the results indicate much less risk of forest damage by the year 2010 (Figure 14). An option has been added into the computer program for directly comparing the estimated areas of risk from two scenarios, in this case that from the 'high' scenario to that from the 'low' scenario (Figure 15). As indicated by Figure 10 the forest area below pH 3.5 in 2030 is estimated three times larger with the 'high' scenario than with the 'low' scenario.
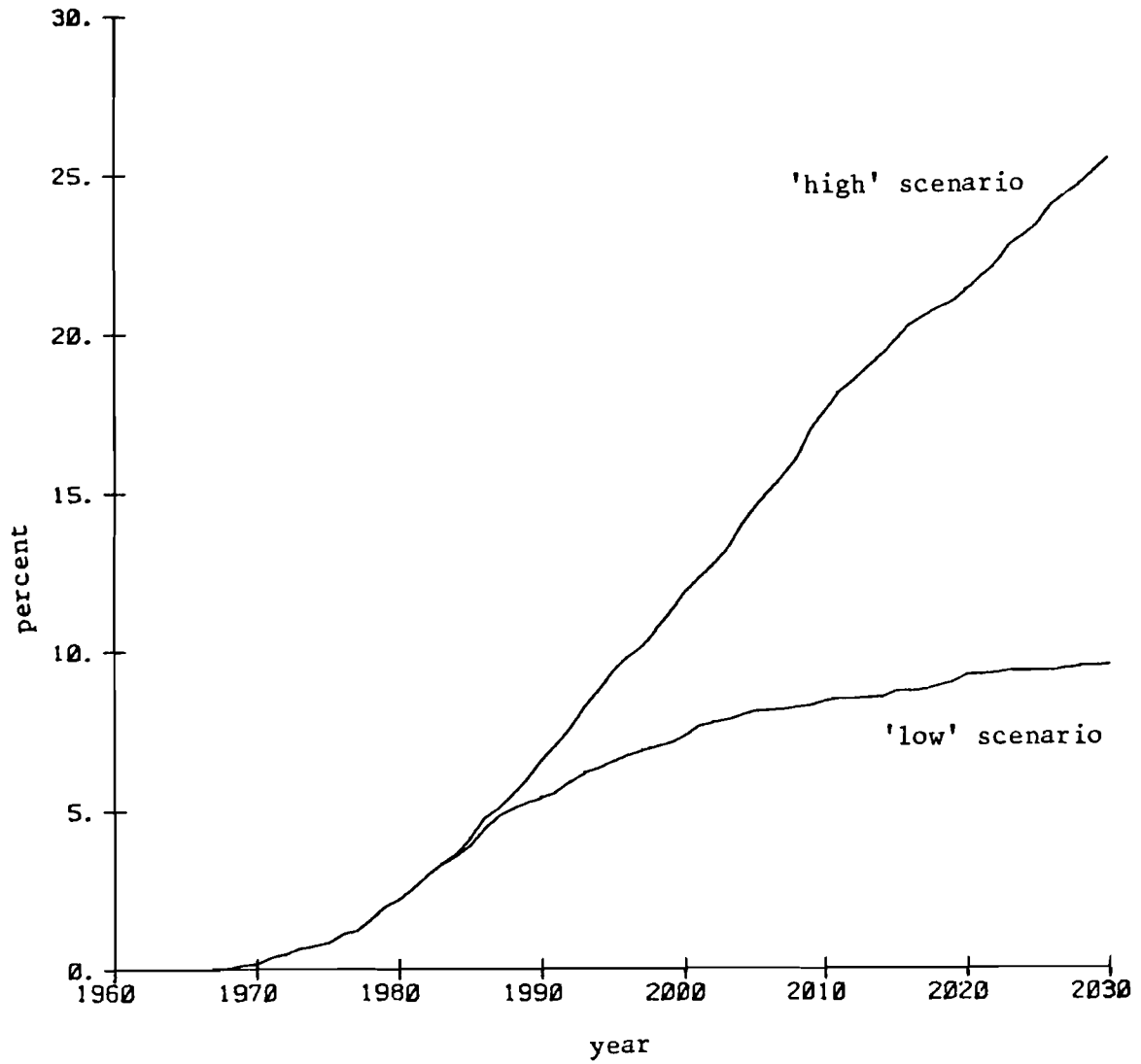
Figure 10 Estimates of the total forest area with soils below pH 3.5 in Europe assuming the two emission scenarios.
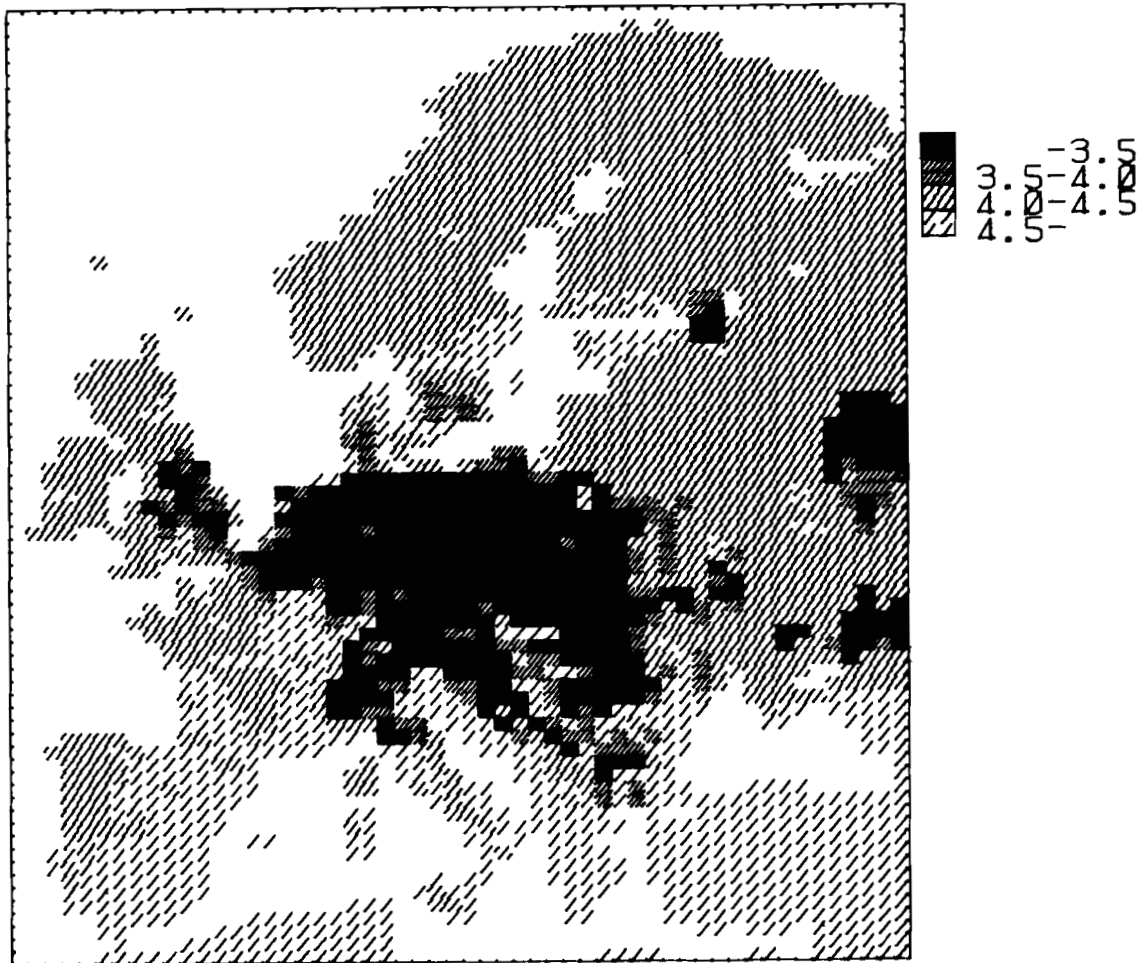
Figure 11.   Model estimates of the soil pH in 2010 assuming the 'high'
              emission scenario.
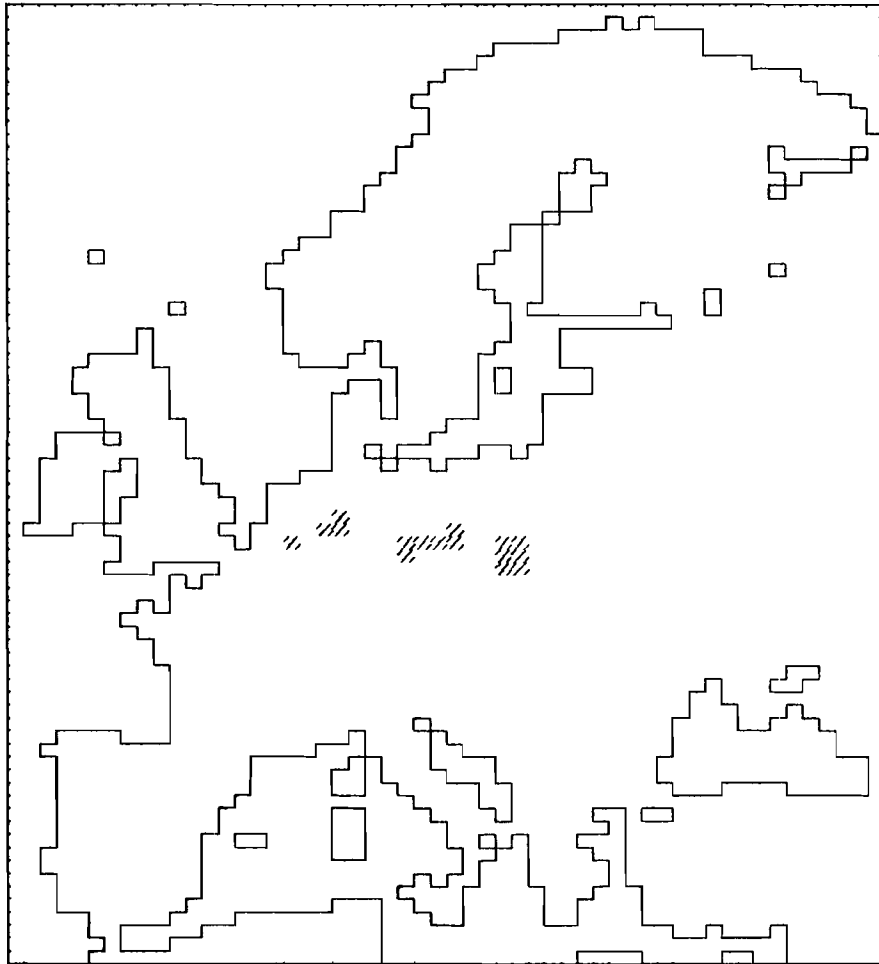
Figure 12.   Model estimates of forest soils below pH 3.5 in 1973.
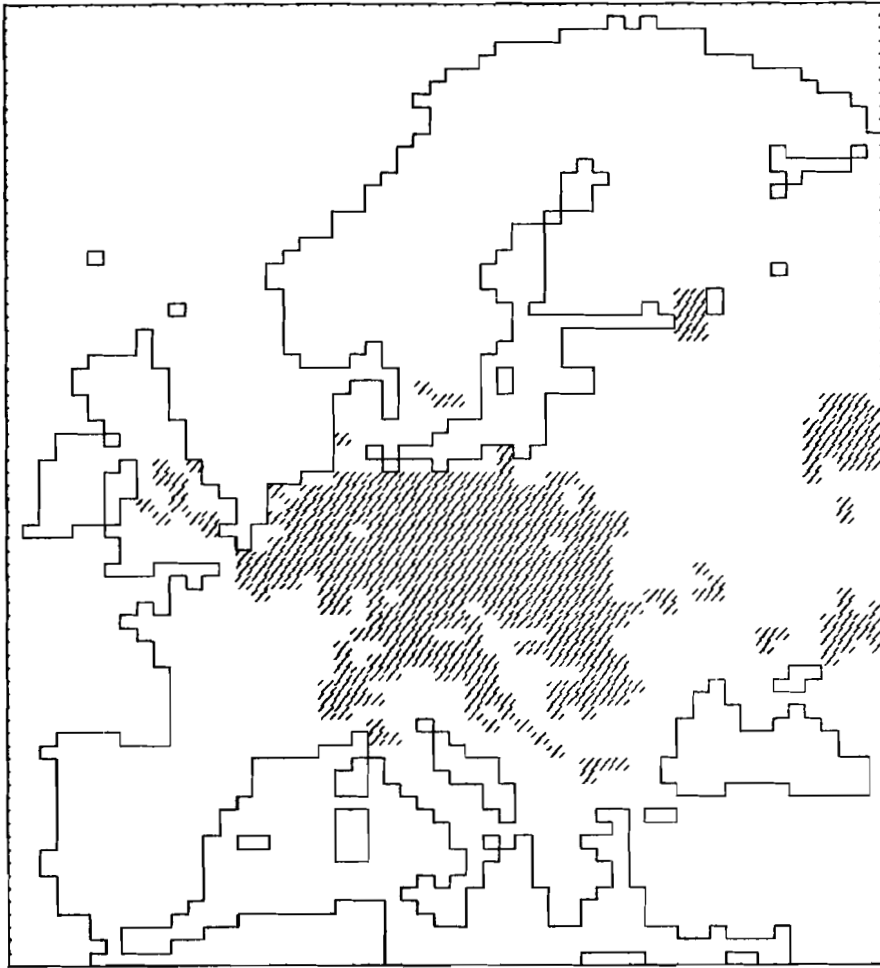
Figure 13.   Model estimates of forest soils below pH 3.5 in 2010 assuming the 'high' emission scenario.
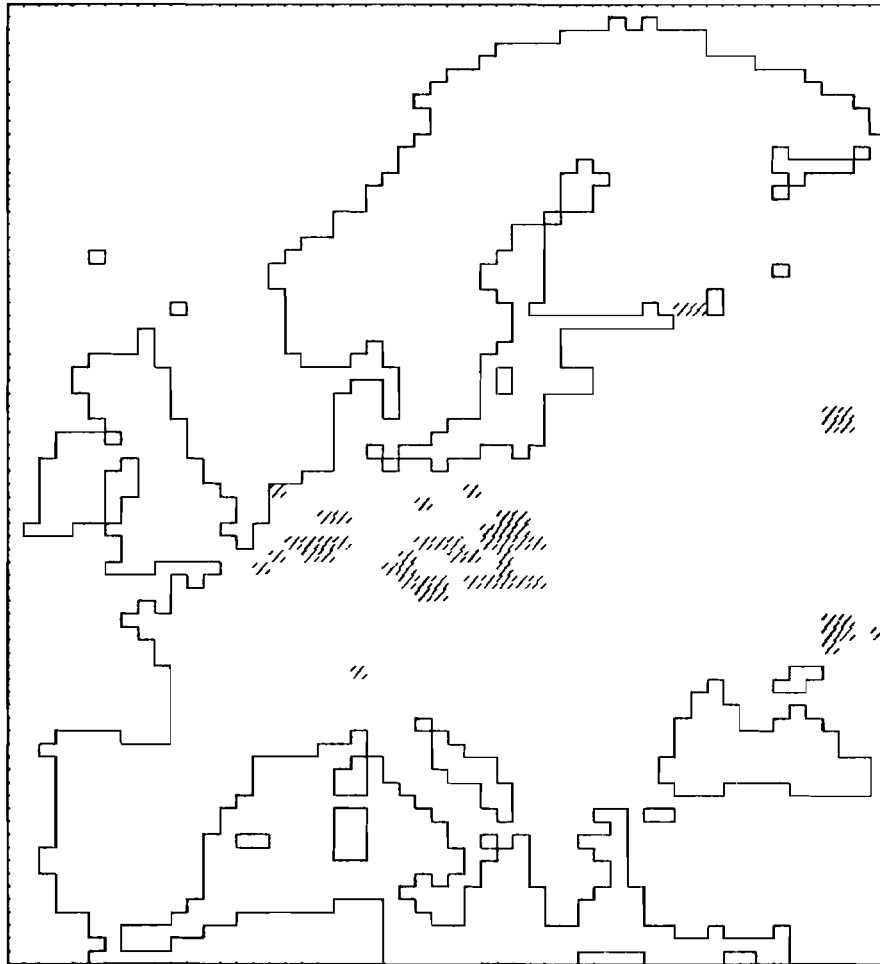
Figure 14.   Model estimates of forest soils below pH 3.5 in 2010 assuming the 'low' emission scenario.
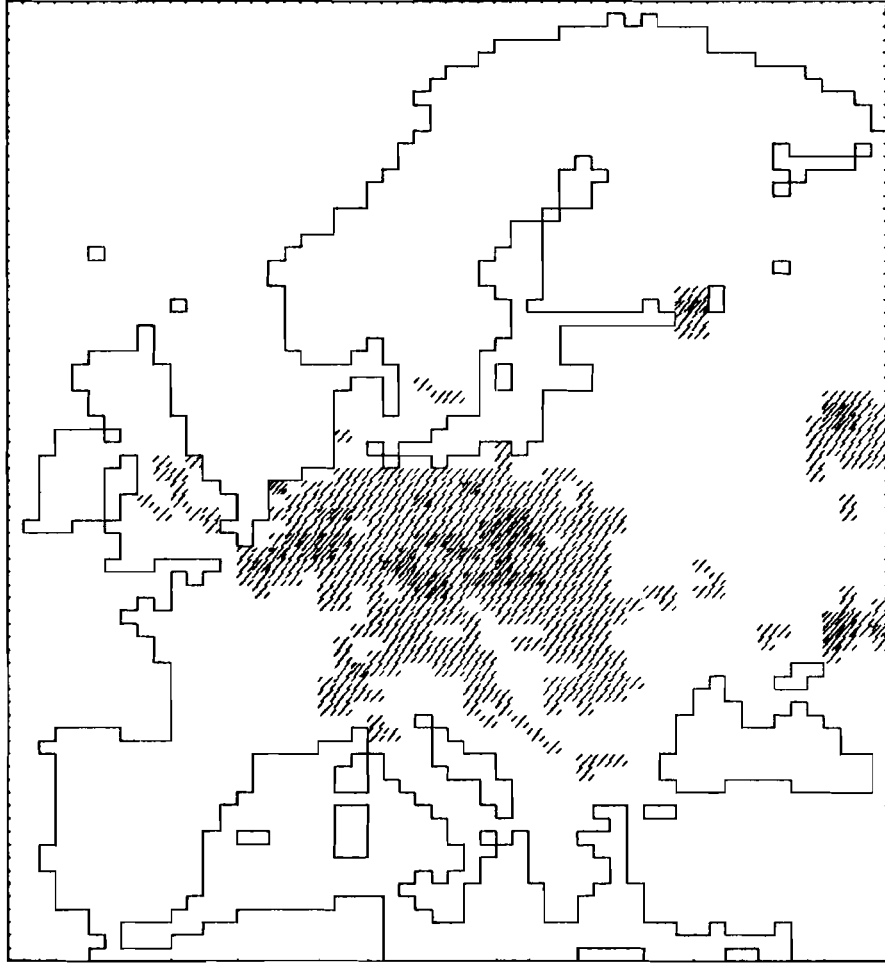
Figure 15.   A comparison of the area of risk in 2010 resulting from the 'high' emission scenario (light shading) and from the 'low' emission scenario (dark shading).

4. Discussion

The model developed in this study can be used for quantifying some aspects of the acidification problem of forest soils which have earlier been discussed using qualitative terms. Many solutions, as they stand now, are crude approximations which need clarification in future research. It is the hope of the authors, however, that the model structure would act as a tool for organizing the data and for identifying research needs. Even in its present stage the model might appear useful in formulating policies to combat the acidification of forest soils in practice.

The model makes a distinction between reversible and irreversible changes in the soil chemistry. Exhaustion of the buffer capacity is more or less irreversible. The case of an insufficient buffer rate, in turn, may be reversible: The buffer rate is again sufficient when the stress rate (annual load) is reduced below a threshold; this threshold is the value of the buffer rate variable. This feature of the model should be useful as it indicates whether a decrease in the acid stress would result in a recovery of the soil, or whether it would merely cause a delay in the acidification process.

The soil acidification model and the application to the European overview are simplifications, which necessarily include uncertainties. The limitations and the different sources of uncertainty are discussed below, first, by addressing the model itself and, then, by focusing on the application.

The model, designed for studies on forest soils, appears too complex for studies on agricultural soils. Intensive agriculture maintains high pH values in soils by means of liming and other practices. In theory, the model could be used for calculating the amount of lime needed to counteract, for example, the acidic deposition. This calculation, however, can be done using more straight-forward methods.

An important indicator variable of the model, facilitating comparisons between scenarios, is the 'critical pH'. The value 3.5 was used, because it was defined as a typical value for the aluminum buffer range, in which there is an increased risk for forest damage. More research would be needed for relating the risk of forest damage to the soil pH. The model could be developed in this respect by replacing the 'critical pH' concept with a continuous s-shaped function for indicating an increase of the risk of forest damage with a decrease in the soil pH.

Soil acidification poses a threat to forest ecosystems and generates predisposing stress in ecosystems as defined by Manion (1981). Forest damage, however, is a multicausal phenomenon. Many factors are involved such as ozone pollution, heavy metals, exceptional climatic conditions, and cultivation of tree species outside of their natural sites. The interactions of soil acidification and the other factors deserve concerted research effort. It does not seem possible today to describe the forest damage in satisfactory detail with any specific model. But emphasizing the complexity of the forest damage as an argument against serious modeling efforts may well cause a delay in obtaining a better understanding of the phenomenon.

The application of the model to the problem of acidic deposition in Europe indicates that soil buffering fails in maintaining adequate pH levels in large parts of Central Europe. In Northern Europe, although the buffering is generally less efficient, the acidic deposition would cause lower rates of acidification compared to those in Central Europe. This does not prove that the problem of soil acidification is restricted to Central Europe. Acidification due to biomass accumulation, i.e. the so-called internal proton production, has a special role in Northern Europe where low temperatures retard biomass decomposition. High internal proton production increases the susceptibility of the environment to the acidification due to air pollutants. This was not taken into account in the above application in its present phase.

The soil variables were initialized for 1960. This does not imply that no acid stress was assumed before that time. The initialization should be viewed as fixing a reference point rather than a manifestation of the state of virgin forests. The initialization should be based on field measurements; in the present application this goal was only partially fulfilled.

Regarding the application there is an additional source of uncertainty: determining the rate of acid stress. Partially this uncertainty is due to the spatial variation and temporal fluctuation of the pollutant composition. Mainly, however, this seems to result from the locally enhanced deposition rates. Forests adsorb pollutants more effectively than open agricultural areas. This feature has not been included into the long range transport models, and it seems certain that the application above uses too low estimates for the acid stress in relatively polluted areas where the stress is largely due to dry deposition.

The reacting volume was fixed at the top 50 cm of the soil. No horizontal gradients were explicitly assumed. Including deeper layers into the reactive part of the soil would add to the reacting volume and it would thus postpone the acidification of soils. Including the gradients would involve faster acidification in the very top of the soil and slower acidification in the deeper layers. The above results correspond to the average situation in the volume. This average value may be inaccurate in some cases due to the nonlinearities of the model. Moreover, the model assumes that all deposition actually reacts within the top soil. This may not always be the case. If part of the deposition flows unchanged in the top soil, the soil response will be delayed and the acidification problem is transferred into the adjacent ecosystems or to the groundwater. An effort is currently under way within the IIASA Acid Rain Project to apply of the soil pH model as a component of a regional model of surface water acidification.

As indicated in this discussion there are many uncertainties involved in the model. Most of them could be systematically studied using field experiments; many existing results are perhaps not adequately taken into account. The IIASA research group would greatly appreciate suggestions for improving the model and the methods of applying it. Nevertheless, it is the hope of the project group that the present results could already assist in facilitating policy decisions. In this respect the soil acidification model should not be viewed as an independent piece of research but as one part of the IIASA model system.

REFERENCES

Alcamo, J., P. Kauppi, M. Posch and E. Runca. 1984. Acid Rain in Europe: A Framework to Assist Decision Making. WP-84-32. IIASA, Laxenburg, Austria

van Breemen, N., Driscoll, C.T., and Mulder, J., 1984. Acidic deposition and internal proton sources in acidification of soils and waters. Nature (London), 307: 599-604.

Lammel, R., 1984. Endgültige Ergebnisse und bundesweite Kartierung der Waldschadenserhebung. AFZ: 340-344.

Manion, P.D., Tree Disease Concepts, Prentice-Hall, 1981.

OECD, 1979. The OECD Programme on Long Range Transport of Air Pollutants. Measurements and Findings. Paris.

Schütt, P. 1977. Das Tannensterben. Der Stand unseres Wissen über eine aktuelle und gefährliche Komplex-Krankheit der Weisstanne (Abies alba). Forstwiss.Centralblatt, 96: 177-186.

Schütt, P., H. Blaschke, E. Hoque, W. Koch, K.J. Lang und H.J. Schuck. 1983. Erste Ergebnisse einer botanischen Inventur des "Fichtensterbens". Forstwiss.Centralblatt, 102: 201-213.

Ulrich, B. 1981. Theoretische Betrachtungen des Ionenkreislaufs in Waldökosystemen. Z. Pflanzenernähr.Bodenkd., 144, 647-659.

Ulrich, B. 1983a. A concept of forest ecosystem destabilization and of acid deposition as driving force for destabilization. In: B. Ulrich and J. Pankrath: Effects of accumulation of air pollutants in forest ecosystems. D. Reidel Publ.Comp., Netherlands.

Ulrich, B. 1983b. Soil acidity and its relation to acid deposition. In: B. Ulrich and J. Pankrath: Effects of accumulation of air pollutants in forest ecosystems. D. Reidel Publ.Comp., Netherlands.

Maps:

Soil Map of the World, Vols. I,V, FAO-Unesco, Paris, 1974.

International Geological Map of Europe and the Mediterranean Region, Bundesanstalt für Bodenforschung Hannover, Unesco Paris, 1972.

Weltforstatlas (World Forestry Atlas), Verlag Paul Parey, Hamburg and Berlin, 1975.

Appendix 1:

Buffer capacities of the carbonate and the cation exchange buffer ranges estimated for the year 1960 by soiltypes of the FAO-Unesco Soil Map of the World (1974). The last column indicates that the buffer rate of the aluminum buffer range was fixed at 2.0 for all soil types.

soiltype	BC_{Ca}	BC_{CE}	br_{Al}
-	keq ha^{-1}		keq ha^{-1} yr^{-1}
Ao	0.	910.0	2.0
Bc	0.	1225.0	2.0
Bd	0.	165.8	2.0
Be	0.	1824.0	2.0
Bg	0.	180.0	2.0
Bh	0.	136.5	2.0
Bk	37500.0	1470.0	2.0
Bv	0.	2210.0	2.0
Ch	0.	390.0	2.0
Ck	28500.0	2535.0	2.0
Cl	0.	419.3	2.0
Dd	0.	136.5	2.0
De	0.	136.5	2.0
Dg	0.	468.0	2.0
E	30000.0	2600.0	2.0
Gd	0.	126.8	2.0
Ge	0.	302.3	2.0
Gh	0.	146.3	2.0
Gm	0.	183.8	2.0
Hc	10500.0	1170.0	2.0
Hg	750.0	1820.0	2.0
Hh	1500.0	321.8	2.0
Hl	0.	312.0	2.0
I	0.	136.5	2.0
Jc	12000.0	315.0	2.0
Je	300.0	1008.0	2.0
Kh	0.	136.5	2.0
Kk	12000.0	1170.0	2.0
Kl	0.	312.0	2.0

(Table continued next page)

soiltype	BC_{Ca}	BC_{CE}	br_{Al}
-	keq ha^{-1}		keq ha^{-1} yr^{-1}
L	0.	150.0	2.0
Lc	4500.0	170.7	2.0
Lf	0.	138.8	2.0
Lg	0.	146.3	2.0
Lk	22500.0	975.0	2.0
Lo	0.	107.3	2.0
Lv	4500.0	1225.0	2.0
Mo	0.	1495.0	2.0
Od	0.	72.0	2.0
Oe	0.	168.8	2.0
Pg	0.	180.0	2.0
Ph	0.	49.0	2.0
Pl	0.	68.3	2.0
Po	0.	78.0	2.0
Pp	0.	239.2	2.0
Qc	150.0	227.5	2.0
Ql	0.	117.0	2.0
Rca	0.	47.3	2.0
Rcb	0.	136.5	2.0
Rcc	0.	857.5	2.0
Re	0.	136.5	2.0
Rx	0.	47.3	2.0
Sg	7500.0	1579.5	2.0
So	0.	1183.0	2.0
Sm	0.	236.3	2.0
Th	0.	127.5	2.0
Tm	0.	136.5	2.0
To	0.	183.8	2.0
Tv	0.	120.0	2.0
U	0.	136.5	2.0
Vc	48000.0	1170.0	2.0
Vp	13500.0	3640.0	2.0
Wd	0.	47.3	2.0
We	0.	1410.5	2.0
Xh	60000.0	1225.0	2.0
Xk	64500.0	1170.0	2.0
Xl	60000.0	910.0	2.0
Xy	60000.0	1225.0	2.0
Zg	22500.0	1225.0	2.0
Zo	22500.0	1225.0	2.0
Bc-Lc	4500.0	685.6	2.0
I-Bc-Lc	2250.0	469.1	2.0
I-Bd	0.	151.2	2.0
I-Be	0.	765.6	2.0
I-Be-Lc	2250.0	533.9	2.0
I-L	0.	149.3	2.0
I-Lc	2250.0	153.6	2.0
I-Lo-Bc	0.	408.5	2.0
I-Po	0.	126.8	2.0
I-Po-Od	0.	108.5	2.0
I-Re-Rx	0.	106.8	2.0
I-U	0.	136.5	2.0
Lo-Lc	2250.0	139.1	2.0

Appendix 2:

The buffer rates of the silicate buffer range.

```
00000000001111111111122222222222333333333344444444445555
1234567890123456789012345678901234567890123456789001234
74                                            2 2               74
73                                         220222220            73
72                                        2222022222220          72
71                                      02222222221111111120      71
70                                     222222222221112222222222    70
69                                   2220222222222212333322311 0    69
68                                 322222222222222211333322322100   68
67                              2222222321223322111134334311 2     67
66                              22222121122212222211222333222       66
65                             22222221112112131113122222022        65
64                             02222222112122221231111 0 2220 2     64
63                             02222122220 21122211110      22      63
62                             01222222220  22212113110 00222        62
61                          002222221122  0222221133000202         61
60                          0121221111222  2212221123200022222      60
59                       002222222212200 22222111111120 1202222     59
58                       02222222221 0122111122112212322222        58
57                      101222221222022211222222110 2222222         57
56           0          0111222221220 212111222211100022222         56
55                      021132222212 2 011111222120220 022222        55
54                      0222222222122  02222222210011200 20022        54
53                      2222221212220 0231211020 0220222022          53
52           0          221113111222 0001000 200 2222222222          52
51                      21122211111220          2222222222          51
50                      211134110122 0 00222222222222222222222      49
49           0          21111 0100122  22222222222222222202222      48
48           0          010 011112   2222222222222222222222         47
47         0020             11111 2      2222222222222222222       46
46       000200             00 11111 2   2222222222222222222       45
45       000222             000 01110    2222222222222222222       44
44       00220             020 01210     2222222222222222222       43
43       00220             0000020      02222222222222222222       42
42        00220                         02222222222222222222       41
41     000 0220             000000      02222222222222222222       40
40     02200020             00 0    00 02222222222222222222       39
39    00220 0220             020 00 0020022222222222222222222      38
38     2222  0222           00022222022222222222222222222222      37
37    0222  02220         0002222222222222222222222222222222      36
36    0222 0222200       222222222222222222222222222222222       35
35    0220 0222220       222222222222222222222222222222222       34
34  000  0022222       002222222222222222222222222222222222      33
33       0022222    002222222223222222222222221 12222222222222     32
32    02202200022222223222231222222222221112222222222222      31
31  000     0222222223221322222222222221 12222222222222      30
30        2 2222222222222122222222222221 2220222222222      29
29        0002222222222221121222222222221222222222220202     28
28     2 22222222222222222222221122222 12222022222200000     27
27  2211122222222222222222111222212222222222222222         26
26  02222222222221022222222222222222222222200222222        25
25  2222222122220222222222222222222222222202220022        24
24  22122222220022222222222222222222222222202020022022     23
23  22221212021122222222222222222222222200002  0222       22
22  22232122202222220222222222222222202 220 20222        21
21  22223212222222202222222222222222222 2022200000       20
20  2222212222222222224222222222222  002 00000        19
19  2222222222222222 222242222222222   22  0000        18
18  0200  22222222222 2222 22224322222220      000     17
17  02222222222222222  2222  222232222222         000    16
16  222222222222    0 222  222222222           0     15
15  222222222222   00 2320 0222222220          0     14
14  012222222220   00  32220 0222222220 0000     0    13
13  01122222222         0222  2222222220000000000000  12
12  2122122220      00  2222 22220 2 0000000000000  11
11  2121122220      00  2200022002 0000000000000  10
10  222222222   22  00  02 0 220 0000000000000    9
9   0222222222       00  20 0220 0000000000000     8
8   0222222222       2  02200 0000000000000      7
7   222212222      0 22  00220 0000000000000      6
6   222222220      2220  020 0000000000000       5
5   20222220   000 020  02 0000000000000       4
4   02200   000000000 00  00 0000000000000      3
3   02   00000000000        00 000 000000       2
2   0  0000000000000           000000          1
1   000000000000000000       0000    00 000000
00000000001111111111122222222222333333333344444444445555
1234567890123456789012345678901234567890123456789001234
```